

Basics of a Quartz Crystal Microbalance

Introduction

This document provides an introduction to the quartz crystal microbalance (QCM) which is an instrument that allows a user to monitor small mass changes on an electrode. The reader is directed to the numerous reviews¹ and book chapters² for a more in-depth description concerning the theory and application of the QCM. A basic understanding of electrical components and concepts is assumed.

The two major points of this document are:

- Explanation of the Piezoelectric Effect
- Equivalent Circuit Models

Explanation of the Piezoelectric Effect

The application of a mechanical strain to certain types of materials (mostly crystals) results in the generation of an electrical potential across that material. Conversely, the application of a potential to the same material results in a mechanical strain – a deformation. Removal of the potential allows the crystal to restore to its original orientation. The igniters on gas grills are a good example of everyday use of the piezoelectric effect. Depressing the button causes the spring-loaded hammer to strike a quartz crystal thereby producing a large potential that discharges across a gap to a metal wire igniting the gas.

Quartz is by far the most widely utilized material for the development of instruments containing oscillators partly due to historical reasons (the first crystals were harvested naturally) and partly due to its commercial availability (synthetically grown nowadays). There are many ways to cut quartz crystal and each cut has a different vibrational mode upon application of a potential. The AT-cut has gained the most use in QCM applications due to its low temperature coefficient at room temperature. This means that small changes in temperature only result in small changes in

frequency. It has a vibrational mode of thickness shear deformation as shown below in Figure 1.

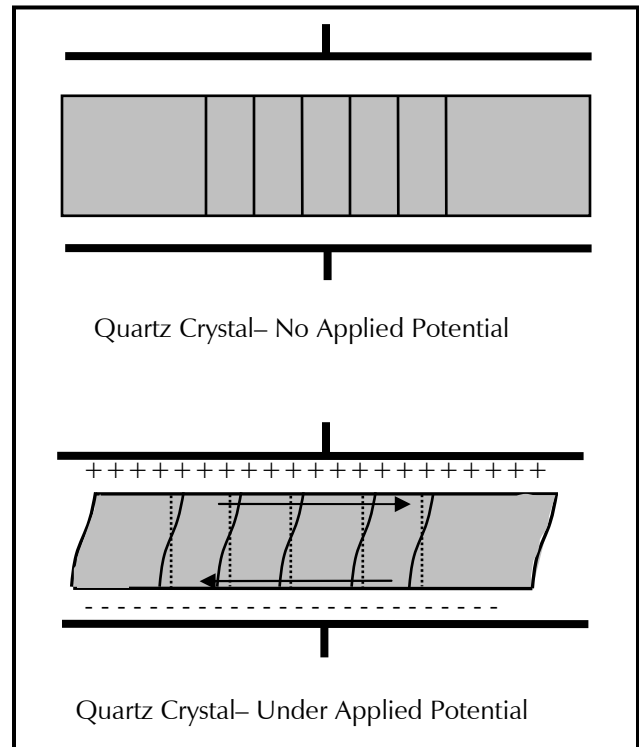


Figure 1. Graphical Representation of Thickness Shear Deformation.

The application of an alternating potential (a sine wave in nearly all cases) to the crystal faces causes the crystal to oscillate. When the thickness of the crystal (t_q) is twice the acoustical wavelength, a standing wave can be established where the inverse of the frequency of the applied potential is $\frac{1}{2}$ of the period of the standing wave. This frequency is called the resonant frequency, f_0 , and is given by the equation

$$f_0 = \sqrt{\frac{\mu_q}{\rho_q}} / 2t_q \quad (1)$$

where μ_q is the shear modulus (a ratio of shear stress to shear strain), ρ_q is the density, and t_q is the crystal thickness. The amount of energy lost during oscillation at this frequency is at a minimum. The ratio of peak energy stored to energy lost per cycle is referred to as the quality factor, Q and is given by the equation

$$Q = \frac{f_c}{\Delta f_{FWHM}} \quad (2)$$

where f_c is the center frequency and Δf_{FWHM} is the full width at half max. This full width at half max is also called the bandwidth. For quartz crystals in air, Q can exceed 100,000 while in solution Q decreases to ~ 3000 . This is because the crystal has been damped by the solution. This damping increases the amount of energy lost per cycle, decreasing Q as shown in Figure 2 below.

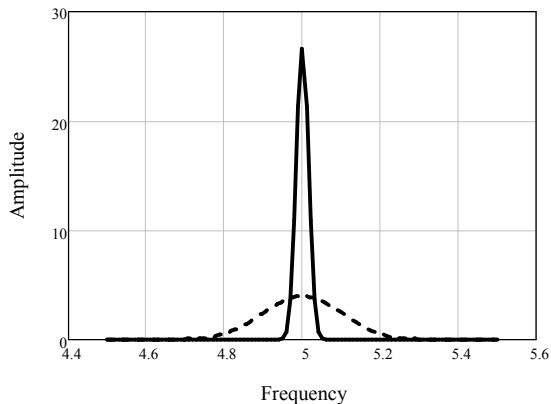


Figure 2. Comparison of High Q and Low Q .

Equivalent Circuit Model

The mechanical model (Figure 3) of an electroacoustical system consists of a mass (M), a compliance (C_m), and a resistance (r_f). The compliance represents energy stored during oscillation and the resistance represents energy dissipation during oscillation.

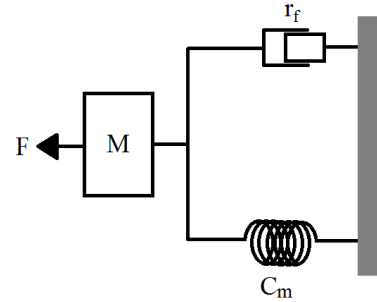


Figure 3. Quartz Crystal Microbalance Equivalent Mechanical Model.

The QCM mechanical model can be electrically modeled in several different ways. The easiest model to understand might be an RLC circuit as shown in Figure 4.



Figure 4. RLC Circuit.

Here R_1 represents the energy dissipated during oscillation, C_1 represents the energy stored during oscillation, and L_1 represents the inertial component related to the displaced mass. At the resonant frequency, f_s , the impedance of the circuit is at a minimum and is equal in magnitude to R_1 as shown in Figure 5.

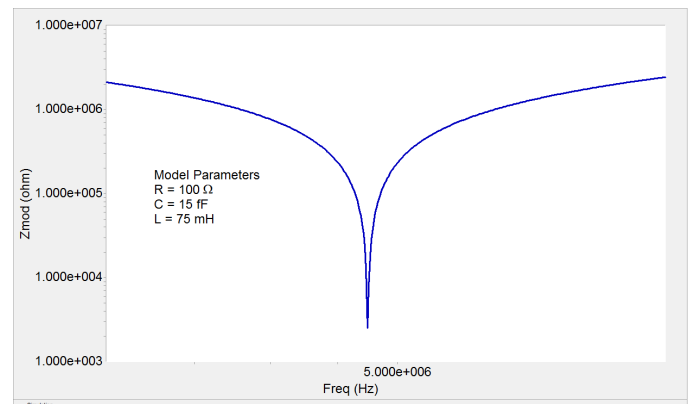


Figure 5. Impedance Spectrum for a Series RLC Circuit.

Making electrical contact to a quartz crystal is most easily done by addition of an electrode to each face of the crystal. These electrodes introduce an additional capacitance (C0) in parallel with the series RLC as shown in Figure 6. This circuit is commonly referred to as the Butterworth – van Dyke (BvD) model.

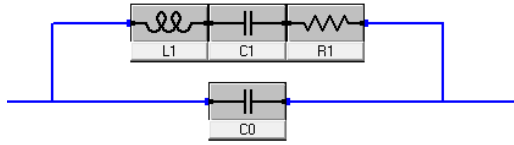


Figure 6. Butterworth – van Dyke Equivalent Circuit Model.

The circuit shown above now has two resonant frequencies, f_s and f_p , which stand for the series resonant frequency (as in the original RLC circuit) and the parallel resonant frequency, respectively. The impedance spectrum for the BvD model is shown below with a minimum at f_s and a maximum at f_p .

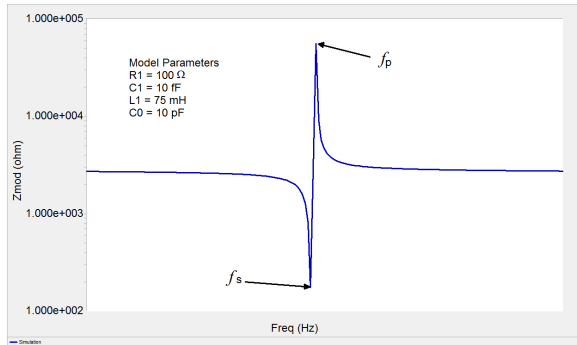


Figure 7. Impedance Spectrum for the Butterworth – van Dyke Equivalent Circuit Model.

Most commercial QCMs that rely upon a phase lock oscillator, manually cancel out C_0 , and only report the series resonant frequency, f_s since $f_s \sim f_0$ and f_s is obviously dependent upon L_1 . It is more accurate to monitor f_p , the parallel resonant frequency since it is more closely associated with a zero-current mechanical model. The eQCM 10M reports both frequencies, f_s and f_p , and a relative impedance spectrum.

Since these two resonant frequencies are dependent upon L_1 , mass changes on the surface of the electrode will result in frequency changes. When a deposited film is thin and rigid, the decrease in frequency can be directly correlated to the increase in mass using the Sauerbrey⁴ equation.

$$\Delta f_{s \text{ or } p} = -\frac{2f_0^2 mn}{(\mu_q \rho_q)^{1/2}} \quad (3)$$

where f_0 is the fundamental frequency of the crystal as defined in Equation (1), m is the mass added, n is the harmonic number (e.g. $n = 1$ for a 5 MHz crystal driven at 5 MHz), and μ_q and ρ_q are as defined above. Equation (3) can be reduced to

$$\Delta f = -C_f m \quad (4)$$

where C_f is the calibration constant. The calibration constant for a 5 MHz At-cut quartz crystal in air is $56.6 \text{ Hz cm}^2 \mu\text{g}^{-1}$.

The majority of electrochemical experiments will correspond to a low-loading case, allowing you to directly correlate changes in frequency with changes in mass using the Sauerbrey equation (4).

Once a film has been deposited and the quartz crystal is immersed in a liquid, the BvD model can be modified as shown below to include coupling to the liquid.

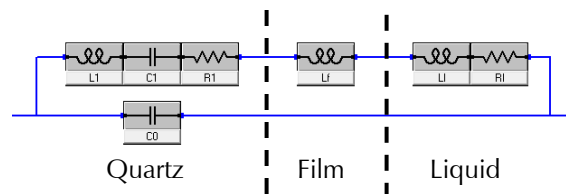


Figure 8. Equivalent Circuit Model for a Quartz Crystal Immersed in a Liquid

Three new components account for the mass loading of the film, L_f , and the liquid loading (based on η_l and ρ_l), L_l and R_l . Both new mass loadings L_f and L_l have the effect of reducing the frequency as indicated with the black arrow in the

chart below. The original BvD model (black curve) shows resonance approximately 300 kHz higher than the modified BvD model (red curve). Notice that the shapes of the resonance curves are identical despite the addition of the film and liquid loading.

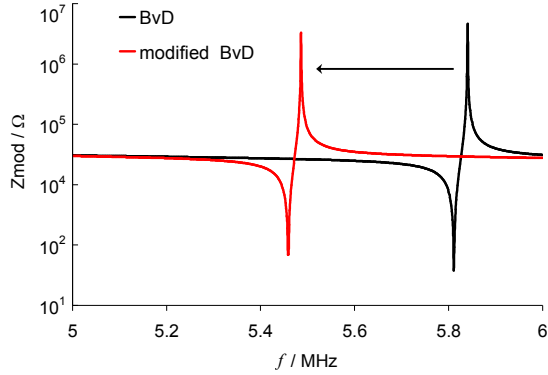


Figure 9. Comparison of BvD and Modified BvD Models.

Knowing the liquid's viscosity and density allows one to calculate³ the expected frequency decrease upon immersing the crystal in that liquid using the equation

$$\Delta f = -f_a^{3/2} \left(\frac{\eta_L \rho_L}{\pi \mu_q \rho_q} \right)^{1/2} \quad (5)$$

where f_a is the frequency of the crystal in air, η_L is the viscosity of the liquid, ρ_L is the density of the liquid, μ_q is the shear modulus of the quartz crystal, and ρ_q is the density of the quartz crystal.

For example, upon immersing the crystal in pure water, a frequency decrease of approximately 800 Hz is expected.

Equation (4) holds as long as the film is assumed to be thin and rigid. When the film is no longer acoustically thin or is not rigid the BvD model can be modified further as shown below.

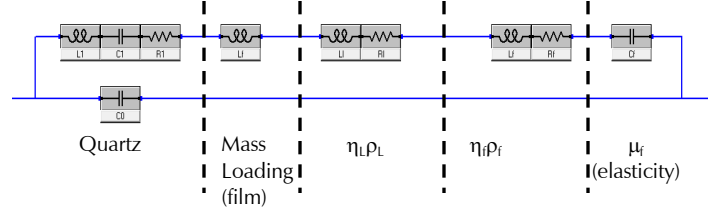


Figure 10. One Possible Equivalent Circuit Model for a Quartz Crystal Coated with a Polymer Film and Immersed in a Liquid

Two new features have been added – Film Loading ($\eta_i \rho_i$) and Elasticity (μ_i). A viscoelastic polymer will influence the resonant frequencies based on the film's viscosity (η_i), density (ρ_i) and elasticity (μ_i). If the polymer is rigid or $\eta_i \rho_i$ does not change during the experiment, there will be no change in peak shape and contributions from $\eta_i \rho_i$ can be ignored. In cases where $\eta_i \rho_i$ does change during the experiment, the frequency, magnitude and shape of the peak will also change as shown in Figure 11.

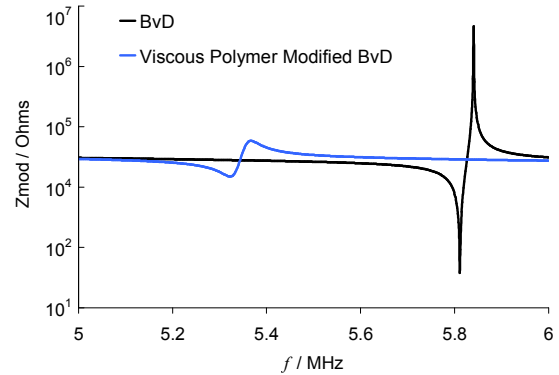


Figure 11. Comparison of BvD and Viscous Polymer Modified BvD Models.

Another way to visualize if $\eta_i \rho_i$ is changing during an experiment is to look at the reduced quality factor, Q_R as a function of time.

$$Q_R = \frac{(f_s + f_p)/2}{(f_p - f_s)} \quad (6)$$

Changes in Q_R correspond to changing $\eta_i\rho_i$.
Quantifying changes in $\eta_i\rho_i$ is challenging
mathematically and will not be explored further

here. The reader is directed to the literature⁵ for
additional information at this time.

Basics of A Quartz Crystal Microbalance. Rev. 1.3 1/13/2011 ©
Copyright 1990-2011 Gamry Instruments, Inc.

References

1. Deakin, M. R.; Buttry, D. A. *Anal. Chem.* **1989**, *61*, 1147A-1154A. Buttry, D. A.; Ward, M. D. *Chem. Rev.* **1992**, *92*, 1355-1379. Buttry, D. A. *Electroanal. Chem.* **1991**, *17*, 1.
2. Buttry, D. A. The Quartz Crystal Microbalance as an In Situ Tool for Electrochemistry, in *Electrochemical Interfaces. Modern Techniques for In-Situ Interface Characterization*, H. D. Abrufia, Ed., VCH Publishers, Inc., New York, **1991**, 531-66. Hillman, A. R. The Electrochemical Quartz Crystal Microbalance. In *Instrumentation and Electroanalytical Chemistry*; Bard, A. J., Stratmann, M., Unwin, P. R., Eds.; Encyclopedia of Electrochemistry; Wiley: New York, **2003**; Vol. 3, 230-289.
3. Glassford, A. P. M. *J. Vac. Sci. Technol.* **1978**, *15*, 1836. Kanazawa, K. K.; Gordon II, J. *Anal. Chem.* **1985**, *57*, 1770. Kanazawa, K. K.; Gordon II, J. *Analytica Chimica Acta* **1985**, *175*, 99-105.
4. Sauerbrey, G. Z. *Phys.* **1959**, *155*, 206.
5. Muramatsu, H.; Tamiya, E.; Karube, I. *Anal. Chem.* **1988**, *60*, 2142-2146. Hillman, A. R.; Jackson, A.; Martin, S. J. *Anal. Chem.* **2001**, *73*, 540-549. Martin; Hillman; Etchnique

